Regime behavior in the SST-cloud forcing relationships over the Pacific cold-tongue region

Chunqiang Wu[1,2*], Tianjun Zhou[1], Rucong Yu[3], De-Zheng Sun[4]

1 LASG, Institute of Atmospheric Physics, Chinese Academy of Sciences, Beijing 100029, China

2 Graduate School of Chinese Academy of Sciences, Beijing 100049, China

3 LaSW, Chinese Academy of Meteorological Sciences, China Meteorological Administration, Beijing 100081, China

4 CIRES, University of Colorado & Earth System Research Laboratory, NOAA 325 Broadway, Boulder, CO 80304, USA

(Submitted to *Geophys. Res. Lett.*)

*Email: wucq@mail.iap.ac.cn

Abstract

Previous studies of water vapor and cloud feedbacks in the tropics usually use observations over the ERBE period (1985-1989) to estimate these feedbacks. Here we extend the analysis to two additional periods: 1990-1994 and 1995-1999. The results show that the values of these feedbacks may depend on which period is chosen for the estimate. The differences in the feedbacks from the long-wave and short-wave forcing of clouds (Cl and Cs) estimated from these three periods are particularly significant. Scatter plots with data from all three periods included indicate a regime behavior in the area-averaged SST-Clouds relationship over the cold-tongue region. The responses of the cirrostratus and deep convective clouds to SST changes exhibit similar behavior as the radiative forcing of clouds. The results suggest that Cloud-SST relationships during ENSO events are nonlinear and may depend strongly on the magnitude as well as the spatial distribution of the surface warming.

1. Introduction

Water vapor and clouds play a vital role in the radiation and heat budget of the Earth-Atmosphere System. They are two major contributors to the greenhouse effect of the Earth's atmosphere. In addition, clouds are a major contributor to Earth's albedo [*Kiehl and Trenberth*, 1997; *Ramanathan and Collins*, 1991]. In response to a naturally or anthropologically produced surface warming, water vapor and clouds can change appreciably to alter radiation fluxes at the top of the atmosphere (TOA), and thereby act as major climate feedbacks that either enhance or reduce the initial warming. The sensitivity of the climate to anthropogenic forcing, such as increase in the CO_2 content in the atmosphere, depends critically on the feedbacks of water vapor and clouds in the climate system [*Manabe and Wetherald*, 1967; *Sun and Lindzen*, 1993]. According to simulations of global warming by general circulation models (GCMs), water vapor feedback is the strongest positive feedback that almost doubling the warming due to the increase in the CO_2 alone. Despite the different parameterization schemes used in the different models, water vapor feedback differs little from one model to another. Feedbacks from clouds, on the other hand, varies greatly among models and are largely responsible for the large spread (about 3^oC) among different models in their estimated equilibrium climate sensitivity to a doubling of CO_2 [*Houghton et al.* 2001, *Colman*, 2003]. Thus, understanding the nature of water vapor and cloud feedbacks still stands a critical issue in the study of global climate change.

Many studies have taken advantage of a natural signal in the climate system-El Niño and South Oscillation (ENSO)-to gain a quantitative understanding of the nature of water vapor and clouds feedbacks [*Ramanathan and Collins*, 1991, *Sun and Trenberth.* 1991, and *Sun et al* 2006, among others]. These studies have fully exploited the satellite observations of water vapor and cloud forcing during the ERBE period [*Barkstrom et al*, 1989]. ERBE only covers the period from 1985 to 1989. Thus, questions about possible nonlinear behavior cannot be addressed as the length of the data is limited. *Senior and Mitchell* [2000] has showed that the climate sensitivity is time-dependent, suggesting feedbacks could depend on the mean background state or the magnitude of warming. *Sun et al.* [2007] found that feedbacks of water vapor and clouds change estimated from the AMIP simulation of ENSO and those estimated from the corresponding coupled simulations of ENSO differ significantly. They pointed out the prevalent cold-bias in the model simulated climatological SST over the equatorial central Pacific may be a factor responsible for the differences. We here focus on the analysis of observations, but use extended data that cover two additional periods that include ENSO events: 1990-1994 and 1995-1999. Our purpose is to check whether feedbacks are different during different El Niño events, and identify any nonlinear or regime behavior that the clouds-SST relationship or water vapor-SST relationship may exhibit.

2. Data and Methodology

In our analysis, the main observational radiative fluxes at TOA are obtained from the NASA World Climate Research Programme/Global Energy and Water-Cycle

Experiment (WCRP/GEWEX) Surface Radiation Budget (SRB) Project [*Stackhouse, et al.,* 2000]. From the aggregate data set for all sites and years, mean bias was determined to be -8.2Wm^{-2}, and the root mean square difference is 23.8Wm^{-2}. TOA heat flux from Earth Radiation Budget Experiment (ERBE) [*Barkstrom et al.*, 1989] is used for comparison. Observations of clouds properties are obtained from the International Satellite Cloud Climate Project (ISCCP) data [*Rossow and Dueñas*, 2004]. The SST used is the Extended Reconstruction SST (ERSST v2) [*Smith and Reynolds,* 2004].

As in *Sun et al.* [2003, 2006], we perform linear regression analysis to calculate feedbacks. In our study, we take the area averaged inter-annual SST anomaly over the entire Pacific cold-tongue region (150^{o}E~110^{o}W, 5^{o}S~5^{o}N) as the forcing (ENSO) signal, and then check how corresponding radiative fluxes at TOA response to the underlying SST anomaly. The reader is referred to *Sun et al.* [2003, 2006] for details of this method. In addition, the greenhouse effect of water vapor （Ga） at TOA are quantified as *Raval and Ramanathan* [1989], the longwave (Cl) and shortwave (Cs) cloud forcing at TOA are defined following *Charlock and Ramanathan* [1985].

3. Result

The SST anomalies (SSTAs) over the entire Pacific cold-tongue region of three El Niño events periods are shown in Fig 1. These three El Niño events periods are defined as the periods from 1985 to 1989, from 1990 to 1994 and from 1995 to 1999, which contains the 1986/87, 1991/92 and 1997/98 El Niño events respectively. We

choose the average over the period from 1985 to 1999 as the climatology, and the monthly SST anomalies were calculated by subtracting the 15-year-mean annual cycle from the original data. As shown in Fig. 1, the 1997/98 El Niño is the strongest El Niño event, the SSTA over the entire Pacific cold-tongue region exceeds about 1.5^{o}C at the end of 1997 and at the beginning of 1998. Compared to the 1997/98 El Niño event, the 1986/87 and 1991/92 El Niño events are much weaker, their SST anomalies did not exceed 1.0^{o}C. Additionally, during 1985/87 El Niño and 1991/92 El Niño, the positive SST anomalies located in the central-eastern equatorial Pacific, but during 1997/98 El Niño the SST anomalies located in the eastern pacific. Another feature of these three periods is that there was a La Niña event followed the El Niño event during the period of 1985-1989 and 199-1999; for the period of 1990-1994, however, there was no La Niña following El Niño. The 1991/92 El Niño was followed by another warm event.

The feedbacks averaged over Pacific cold-tongue region during three periods are quantified and tabulated in Table 1. Besides the results from SRB, that from ERBE over the ERBE period is also listed for comparison. The comparison between ERBE and SRB over the ERBE period shows that feedbacks estimated from these two date sets matched reasonably well. The differences of feedbacks from Cs and Cl between ERBE and SRB are both within the error bar. The difference of Ga is larger, which may be due to the fact that ERBE underestimates the changes of Ga from La Niña to El Niño [*Sun et al.*, 2006]. In general, the consistency between SRB and ERBE gives us confidence to extend this analysis to other periods. The feedbacks

87 estimated for 1990-1994 differ from that of 1985-1989 significantly. The feedbacks
88 from Ga, Cl and Cs all are about 5 $Wm^{-2}K^{-1}$ larger than that for 1985-1989, which all
89 exceed the error bar of estimations. The estimates of 1995-1999 are much similar to
90 that of 1985-1989, and are different from that of 1990-1994.

91 Grouping the data from all these three periods, we have produced scatter
92 diagrams showing the RF-SSTA relationship (Fig. 2). Plotted are interannual
93 anomalies averaged over the entire equatorial cold-tongue region. The variability in
94 Ga apparently is more tightly controlled by variability in SSTA than the variability in
95 Cl and Cs. Within the entire range of the SST variability showed here, a SST increase
96 results in a significant increase in Ga. In contrast, the responses of Cl and Cs to SST
97 appear to be divided into three regimes. When SSTA is below -0.5^{o}C, both Cl and Cs
98 are not sensitive to SSTA (regime I). When SSTA is within -0.5^{o}C to 2.0^{o}C, both Cl
99 and Cs increase with SSTA dramatically (regime II). However, when SST anomaly
100 exceeds 2.0^{o}C, both Cl and Cs decrease with SSTA (regime III). Fig. 2 explains why
101 the feedbacks of Cl and Cs from period of 1990-1994 are much stronger than that of
102 other two periods. During 1990-1994, there is no La Niña event and also the El Niño
103 event is much weaker than 1997/98 El Niño, so SSTA is within the range from -0.5^{o}C
104 to 2.0^{o}C, a range when both Cl and Cs are sensitive to SSTA. However, the period
105 from 1985 to 1989 covers SST anomaly bellow -0.5^{o}C, and the period from 1995 to
106 1999 covers the whole range of the SST anomaly.

107 Further analysis of the corresponding total SST in the central equatorial Pacific
108 during the three regimes suggest that the lack of sensitivity in regime I is linked to the

109 fact that the equatorial central Pacific has to be warm enough to support deep
110 convection. Regime I corresponds to a La Niña situation and the equatorial central
111 Pacific is too cold to support deep convection. Regime II corresponds to an equatorial
112 central Pacific that supports deep convection. The marked increase in the sensitivity in
113 stage II reflects the sensitivity of deep convection in the equatorial central Pacific to
114 changes in the SST in that region. Regime III corresponds to an exceptionally strong
115 warm event that has a maximum of SST warming in the far eastern Pacific. The
116 warming in the coastal region may reduce the moisture convergence to the equatorial
117 central Pacific where deep convection takes place. Composite analysis shows that
118 large positive SSTA during 1985-1989 and 1990-1994 are located in the
119 central-eastern Pacific, but the positive SSTA is located in the eastern Pacific during
120 the period of 1995-1999. During 1995-1999, even most of the basic SST exceeds the
121 convective threshold temperature (~27^{o}C), deep convection averaged over the entire
122 equatorial cold-tongue region is still suppressed. It further shows that the responses of
123 RFs to SST are linked to the total SST in the equatorial central Pacific as well as the
124 magnitude of warming in the far eastern Pacific. The latter determines changes in the
125 SST gradients over that region and therefore large-scale circulation. *Bony et al*. [1997]
126 also underscored the role of large-scale circulation in determining response of cloud
127 forcing to SST changes.

128 To understand how this response of Cl and Cs to SSTA is linked to the response
129 of the vertical structures of clouds to SSTA over Pacific cold-tongue region, we
130 further employed data from ISCCP D2 [*Rossow and Dueñas*, 2004] and quantified the

131 climatology of clouds properties and their response to SST anomalies. *Cess et al.*
132 [2001a, b] showed the influence of 1998 El Niño on the RF and cloud structure over
133 the west Pacific warm pool region. How does the El Niño events affect the radiative
134 forcing and cloud structure over Pacific cold-tongue region is not yet known. On
135 average, low level cloud is dominant over Pacific cold-tongue region, with a value
136 about 26.1%. The high level cloud is slightly less, with a value of 23.4%. The high
137 level clouds can divided into cirrus, cirrostratus and deep convective could, the
138 amount of cirrus is largest (17.8%), and the sum of cirrostratus and deep convective
139 could is 8.1%. The amount of middle level cloud is 11.53%. Radiative forcing of
140 clouds is a function of cloud types. To further understand the regime behavior shown
141 in Fig. 2, we further plotted scatter diagrams of cloud optical thickness versus SSTA,
142 cloud-top temperatures versus SSTA, cirrus cloud versus SSTA, cirrostratus and deep
143 convective clouds versus SSTA, middle level clouds versus SSTA, and the low level
144 clouds versus SSTA. The response difference in cloud radiative forcing in different
145 ranges of SSTA may be explained by the changes of optical thickness and cloud top
146 temperature in different ranges of SSTA (fig 3a, 3b). Both optical thickness and cloud
147 top temperature have two significant changes in their slopes with respect to SSTA.
148 Two significant changes in the slope are also found the scatter plot of cirrostratus and
149 deep convection clouds versus SSTA. The cirrus-formed mostly from the detrainment
150 of deep convective clouds, and the total middle level cloud amount are found to
151 increase with SSTA in a more or less monotonically. The slope between the low level
152 clouds and SSTA remains almost unchanged until the SSTA exceeds 2.0^{o}C. So Fig.

153 3c, 3e, and 3f suggest that contributions from the low and middle level clouds and
154 cirrus to the regime behavior in Fig. 2 may be small.

155 4. Summary

156 Using radiative fluxes at TOA from SRB, we estimate feedbacks from water
157 vapor greenhouse effect (Ga), long wave cloud radiative forcing (Cl) and short wave
158 cloud radiative forcing (Cs) over 1990-1994 and 1995-1999 and compared with the
159 results from the more commonly used ERBE period (1985-1989). We have found
160 significant differences in the estimates from these different periods, particularly in the
161 estimates of the cloud feedbacks. These differences are explained by the differences in
162 the magnitude as well as the distribution of the SST anomalies in these three different
163 periods. Averaged over the entire cold-tongue region, the cloud forcing and SST
164 relationship exhibit a regime behavior--three different relationships are observed as
165 the SST anomaly over the cold-tongue changes from strongly negative to strongly
166 positive. Similar regime behavior is also noted in the corresponding scatter diagrams
167 of cirrostratus and deep convection cloud versus SST. In the near future, we plan to
168 expand the study of *Sun et al*. [2006] which focused on the ERBE period only, to
169 these two additional periods that also have ENSO events, to check whether the models
170 could produce any regime behavior in the cloud forcing and SST relationships. With
171 the present results, we also believe that assuming a linear relationship between cloud
172 forcing and SST in quantifying cloud feedbacks, either in observations, or in model
173 simulations, may be an oversimplification.

References:

Barkstrom, B., E. Harrison, G. Smith, R. Green, J. Kibler, R. Cess, and the ERBE Science Team(1989): Earth Radiation Budget Experiment (ERBE) Archival and April 1985 Results. *Bull. Amer. Meteor. Soc.*, *70***,** 1254-1262.

Bony, S., K. Lau, and Y. C. Sud (1997): Sea Surface Temperature and Large-Scale Circulation Influences on Tropical Greenhouse Effect and Cloud Radiative Forcing. *J. Clim.*, *10***,** 2055-2077.

Cess, R. D. and G. L. Potter (1988): Methodology for understanding and intercomparing atmospheric climate feedback processes in general circulation models. *J. Geophys. Res.*, *93***,** 8305-8314.

Cess, R. D., G. L. Potter, J. P. Blanchet, G. J. Boer, and A. D. Genio (1990): Intercomparison and interpretation of climate feedback processes in 19 atmospheric general circulation models. *J. Geophys. Res.*, *95***,** 16,601 – 16,615.

Cess, R. D*., et al.* (1996): Cloud feedback in atmospheric general circulation models: An update. *Geophys. Res. Lett.*, *101***,** 12791-12794.

Cess, R. D., M. Zhang, P. Wang, and B. A. Wielicki (2001a): Cloud structure anomalies over the tropical Pacific during the 1997/98 El Niño. *Geophys. Res. Lett.*, *28***,** 4547 – 4550.

Cess, R. D., M. Zhang, B. A. Wielicki, D. F. Young, X. L. Zhou, and Y. Nikitenko (2001b): The Influence of the 1998 El Niño upon Cloud-Radiative Forcing over the

Pacific Warm Pool. *J. Clim.*, *14*, 2129-2137.

Charlock, T. P. and V. Ramanathan (1985): The Albedo Field and Cloud Radiative Forcing Produced by a General Circulation Model with Internally Generated Cloud Optics. *J. Atmos. Sci.*, *42*, 1408-1429.

Colman, R. (2003): A comparison of climate feedbacks in general circulation models. *Clim. Dyn.*, *20*, 865-873.

Kiehl, J. T. and K. E. Trenberth (1997): Earth's Annual Global Mean Energy Budget. *Bull. Amer. Meteor. Soc.*, *78*, 197-208.

Manabe, S. and R. T. Wetherald (1967): Thermal Equilibrium of the Atmosphere with a Given Distribution of Relative Humidity. *J. Atmos. Sci.*, *24*, 241-259.

Ramanathan, V. and W. Collins (1991): Thermodynamic regulation of ocean warming by cirrus clouds deduced from observations of the 1987 El Niño. *Nature*, *351*, 27-32.

Rossow, W. B. and E. N. Dueñas (2004): The International Satellite Cloud Climatology Project (ISCCP) Web Site: An Online Resource for Research. *Bull. Amer. Meteor. Soc.*, *85(2)*, 167-172.

Senior, C. A. and J. F. B. Mitchell (2000): The time-dependence of climate sensitivity. *Geophys. Res. Lett.*, *27*, 2685-2688.

Smith, T. M. and R. W. Reynolds (2004): Improved Extended Reconstruction of SST (1854-1997). *J. Clim.*, *17*, 2466-2477.

41 Stackhouse, P. W., S. K. Gupta, S. J. Cox, M. Chiacchio and J. C. Mikovitz (2000):
42 The WCRP/GEWEX Surface Radiation Budget Project Release 2: an assessment of
43 surface fluxes at 1 degree resolution. In: Smith WL, Timofeyev Y (eds) IRS 2000:
44 Current problems in atmospheric radiation. International Radiation Symposium,St.
45 Petersburg, Russia, July 24–29, 2000

46 Soden, B. J., A. J. Broccoli, and R. S. Hemler (2004): On the Use of Cloud Forcing to
47 Estimate Cloud Feedback. *J. Clim.*, *17***,** 3661-3365.

48 Sun, D. Z. and R. S. Lindzen (1993): Wator vapor feedback and the ice age snowline
49 record. *Ann. Geophys.*, *11***,** 204-215.

50 Sun, D. Z. and K.E. Trenberth (1998): Coordinated heat removal from the equatorial
51 Pacific during the 1986-87 El Niño. *Geophys. Res. Lett., 25*, 2659-2662

52 Sun, D. Z., J. Fasullo, T. Zhang, and A. Roubicek (2003): On the Radiative and
53 Dynamical Feedbacks over the Equatorial Pacific Cold Tongue. *J. Clim.*, *16,*
54 2425-2432.

55 Sun, D. Z., T. Zhang, C. Covey, S. A. Klein, W. D. Collins, J. J. Hack, J. T. Kiehl, G.
56 A. Meehl, I. M. Held, and M. Suarez (2006): Radiative and Dynamical
57 Feedbacks over the Equatorial Cold Tongue: Results from Nine Atmospheric
58 GCMs. *J. Clim.*, *19,* 4059-4075.

59 Sun, D. Z., Y. Q. Yu, and T. Zhang, 2007: Tropical Water Vapor and Cloud
60 Feedbacks in Climate Models: A Further Assessment Using Coupled Simulations.
61 *J. Clim*., Submitted**.**

62 Wetherald, R. T. and S. Manabe (1988): Cloud feedback processes in a general
63 circulation model. *J. Atmos. Sci.*, *45***,** 397-1415.

Table. 1. The estimations of feedbacks over the equatorial central Pacific (5^oS~5^oN,150^oE~110^oW) from water vapor greenhouse effect (Ga), long wave cloud radiative forcing (Cl) and short wave cloud forcing(Cs). The values of these feedbacks are obtained through a linear regression using the inter-annual variations of the SST and corresponding fluxes over the equatorial central Pacific.

Feedbacks (Wm^{-2}/K)				
Name Of Processes	85 to 89		90 to 94	95 to 99
	ERBE	SRB	SRB	SRB
$\frac{\partial Ga}{\partial T}$	6.75± 0.27	7.50± 0.29	12.03± 0.93	9.63± 0.46
$\frac{\partial Cl}{\partial T}$	11.82± 0.97	10.97± 0.81	15.85± 2.05	12.44± 0.61
$\frac{\partial Cs}{\partial T}$	-10.57± 1.21	-10.40± 0.92	-16.89± 2.67	-13.26± 0.89

Figure captions

Fig. 1. (a) Time series of SST anomalies for the period 1985-1989 (solid line), 1990-1994 (dotted line), and 1995-1999 (long-dashed line) over Pacific cold-tongue region (5^{o}S-5^{o}N, 150^{o}E-110^{o}W). The SST used is from ERSST V2 (Smith and Reynolds, 2004) (b) Spatial pattern of composite positive SST anomalies for these three different periods.

Fig. 2. Scatter diagrams showing the relationship between a) water vapor greenhouse effect, b) longwave cloud radiative forcing, c) shortwave cloud radiative forcing and d) net cloud radiative forcing anomaly and SST anomaly on the inter-annual time scale for three period: period from 1985 to 1989 (blue dots), period from 1990 to 1994 (red dots) and period from 1995 to 1999 (green dots). Each dot corresponds to one grid within the domain (5^{o}S-5^{o}N, 150^{o}E-110^{o}W) at T42 resolution.

Fig. 3. Scatter diagrams showing the relationship between a) cloud optical thickness, b) cloud-top temperature, c) cirrus cloud, d) sum of cirrostratus and deep convection cloud, e) sum of middle level clouds and f) sum of low level clouds and SST anomaly. The cloud properties are derived from ISCCP D2 data and based on T42 monthly means data during 1985 to 1999 over Pacific cold-tongue region.

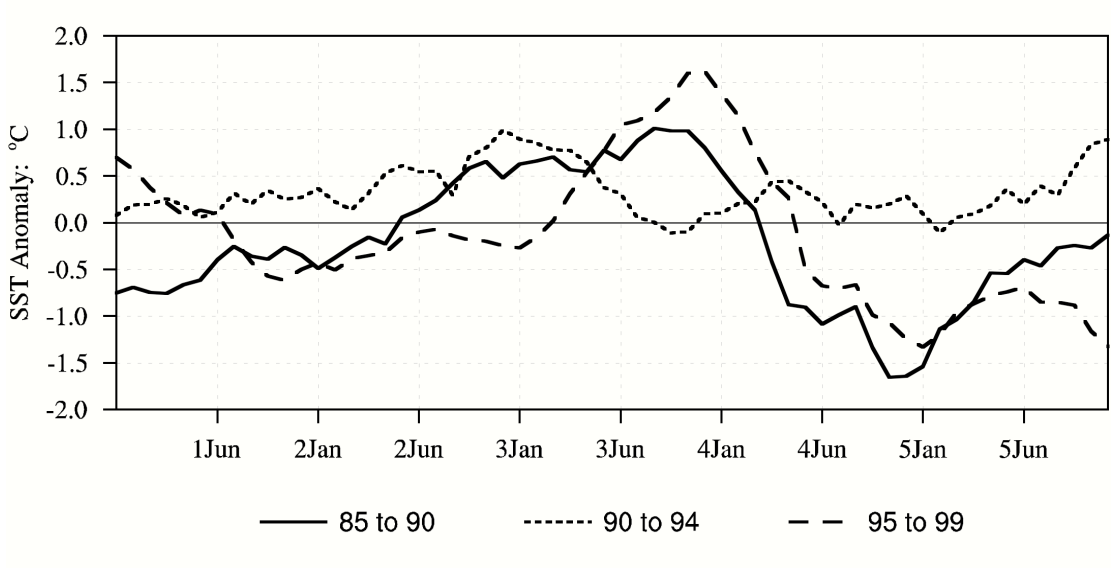

Fig. 1. Time series of SST anomalies for the period 1985-1989 (solid line), 1990-1994 (dotted line), and 1995-1999 (long-dashed line) over Pacific cold-tongue region (5^{o}S-5^{o}N, 150^{o}E-110^{o}W). The SST used is from ERSST V2 (Smith and Reynolds, 2004)

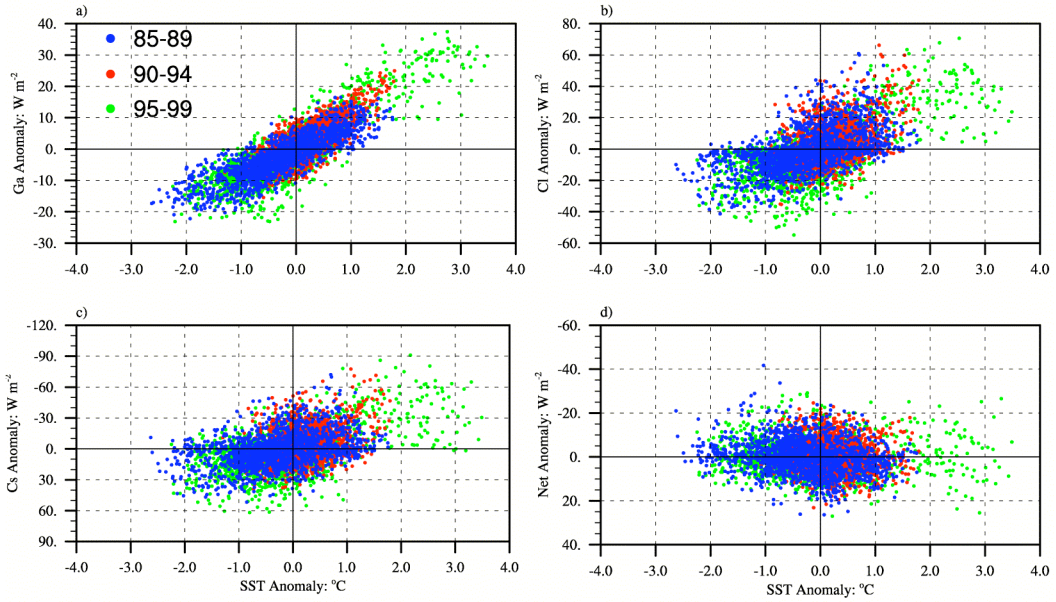

Fig. 2. Scatter diagrams showing the relationship between a) water vapor greenhouse effect, b) longwave cloud radiative forcing, c) shortwave cloud radiative forcing and d) net cloud radiative forcing anomaly and SST anomaly on the inter-annual time scale for three period: period from 1985 to 1989 (blue dots), period from 1990 to 1994 (red dots) and period from 1995 to 1999 (green dots). Each dot corresponds to one grid within the domain (5°S-5°N, 150°E-110°W) at T42 resolution.

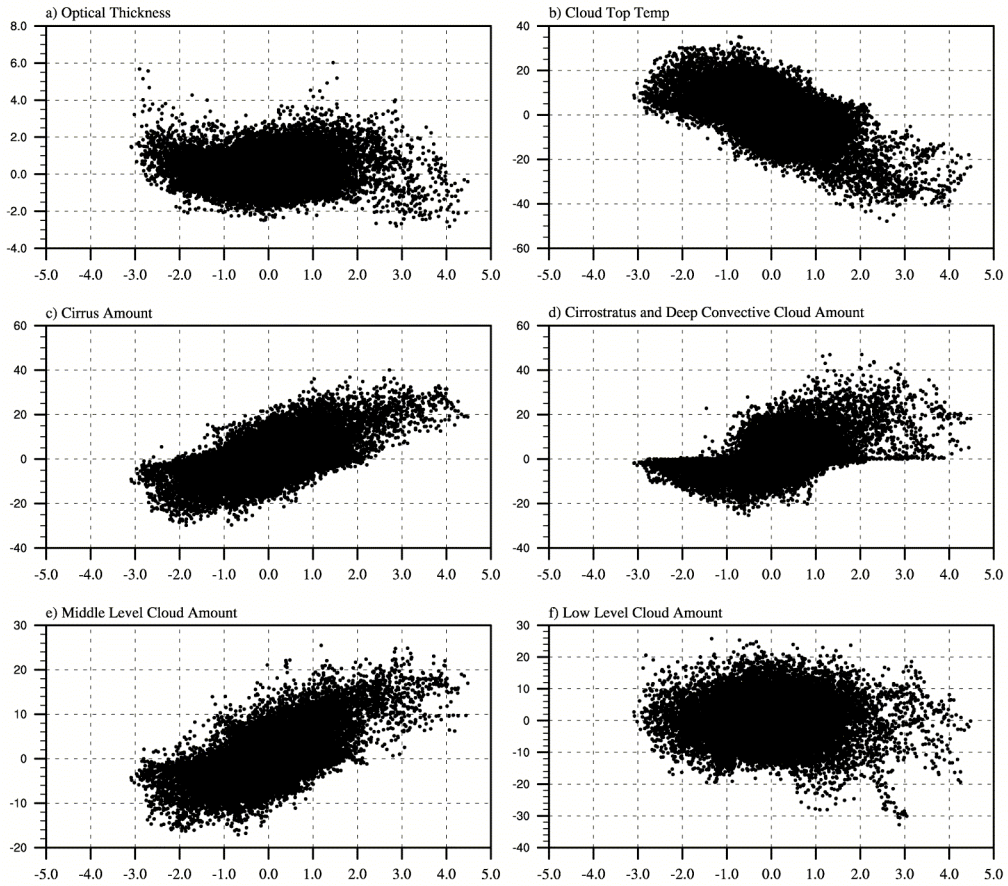

Fig. 3. Scatter diagrams showing the relationship between a) cloud optical thickness, b) cloud-top temperature, c) cirrus cloud, d) sum of cirrostratus and deep convection cloud, e) sum of middle level clouds and f) sum of low level clouds and SST anomaly. The cloud properties are derived from ISCCP D2 data and based on T42 monthly means data during 1985 to 1999 over Pacific cold-tongue region.